This article has been accepted for inclusion in a future issue of this journal. Content is final as presented, with the exception of pagination.

An Adaptive Wearable Parallel Robot for the Treatment of Ankle Injuries

Prashant K. Jamwal, Sheng Q. Xie, *Senior Member, IEEE*, Shahid Hussain, and John G. Parsons

***Abstract*—This paper presents the development of a novel adaptive wearable ankle robot for the treatments of ankle sprain through physical rehabilitation. The ankle robot has a bioinspired design, devised after a careful study of the improvement opportunities in the existing ankle robots. Robot design is adaptable to subjects of varying physiological abilities and age groups. Ankle robot employs lightweight but powerful pneumatic muscle actuators (PMA) which mimics skeletal muscles in actuation. To address nonlinear characteristics of PMA, a fuzzy-based disturbance observer (FBDO) has been developed. Another instance of an adaptive fuzzy logic controller based on Mamdani inference has been developed and appended with the FBDO to compensate for the transient nature of the PMA. With the proposed control scheme, it is possible to simultaneously control four parallel actuators of the ankle robot and achieve three rotational degrees of freedom. To evaluate the robot design, the disturbance observer, and the adaptive fuzzy logic controller, experiments were performed. The ankle robot was used by a neurologically intact subject. The robot–human interaction was kept as active–passive while the robot was operated on predefined trajectories commonly adopted by the therapists. Trajectory tracking results are reported in the presence of an unpredicted human user intervention, use of compliant and nonlinear actuators, and parallel kinematic structure of the ankle robot.**

***Index Terms*—Adaptive fuzzy logic controller, fuzzy-based disturbance observer (FBDO), pneumatic muscle actuators (PMAs), wearable ankle rehabilitation robot.**

I. Introduction

THE ankle joint is a complex structure in the human musculoskeletal system and plays an important role in maintaining body balance during ambulation [1], [2]. Due to its location, the human ankle is frequently subjected to large loads which can reach up to several times of the body weight. The exposure to such large loads also means a higher likelihood of injuries. In fact, the ankle is the most common site of sprain injuries in the human body, with over 23 000 cases per day in the U.S. [3]. Ankle sprains are injuries that involve the overstretching or tearing of ligaments around the ankle and are often sustained during sporting or acts of daily living. Ankle sprains can be classified into several grades, ranging from mild overstretching to complete disruption of ankle ligaments. Depending on the severity of the sprain, the time required for recovery can range from 12 days to more than six weeks [4]. Researchers have reported that a significant number (>40%) of severe ankle sprains can develop into chronic ankle instability [4], [5], which makes the ankle more susceptible to further injuries in the future. Furthermore, there is considerable evidence following ankle injury of prolonged symptoms [6], [7], self-reported disability [7], diminished physical activity [8], and recurrent injury [9] are commonly reported for months and years after initial injury. There is also emerging evidence linking severe and repetitive ankle sprains to the development of ankle osteoarthritis [10], [11]. Functional instability of the ankle joint often results and is typically ascribed to sensorimotor, or neuromuscular, deficits that accompany ligamentous injury.

The general rehabilitation program for ankle sprains is carried out in stages. The initial stage of treatment right after injury is considered the acute phase of rehabilitation and is focused on reducing effusion and swelling at the affected to promote healing of the injured tissues. A reduction in effusion can be achieved with elevation, application of ice, and compression. The affected ankle is also often immobilized. However, as prolonged immobilization of the ankle can lead to reduced range of motion (ROM), compounding of sensorimotor deficits and muscular atrophy, the next phase of ankle rehabilitation typically involves ROM and muscle strengthening exercises. ROM exercises are normally carried out within the pain-free range of the patient to improve the ROM and reduce muscular atrophy. Research has also suggested that this has the ability to stimulate healing of torn ligaments [4]. The muscle strengthening phase is achieved once pain free weight bearing gait is possible. During this phase, ROM exercises are continued together with the commencement of muscle stretching and resistive exercises [4]. The resistance level of these strengthening exercises should be increased as the patient progresses with recovery. Muscle stretching is important to assist the recovery of joint ROM while resistance training is used to improve the strength of muscles surrounding the ankle to prevent future injuries [12]. Finally, proprioceptive and balancing exercises should be carried out toward the end of the rehabilitation program (functional phase) to enhance the patients' sense of joint position, thus giving them better foot and ankle coordination and improving their ability to respond to sudden perturbations at the ankle [4] and minimize the risk of further injury [13].

It has been documented that using conventional approaches, the recuperation is slow and tedious [14]. It is apparent from

Manuscript received June 18, 2011; revised November 29, 2011, March 20, 2012, and July 8, 2012; accepted September 5, 2012. Recommended by Technical Editor S. Martel. This work was supported by the National Natural Science Foundation of China under Grant 50975109.

P. K. Jamwal is with Rajasthan Technical University, Kota 324010, India (e-mail: pjam025@aucklanduni.ac.nz).

S. Q. Xie and S. Hussain are with the School of Engineering, The University of Auckland, Auckland 1142, New Zealand (e-mail:s.xie@auckland.ac.nz; shus045@aucklanduni.ac.nz).

J. G. Parsons is with the School of Nursing, The University of Auckland, Auckland 1142, New Zealand (e-mail: j.parsons@auckland.ac.nz).

Color versions of one or more of the figures in this paper are available online at http://ieeexplore.ieee.org.

Digital Object Identifier 10.1109/TMECH.2012.2219065

1083-4435/$31.00 © 2012 IEEE

This article has been accepted for inclusion in a future issue of this journal. Content is final as presented, with the exception of pagination.

earlier discussion that muscular strength and good proprioception are vital in preventing functional instability in the ankle. Emphasis must, therefore, be placed in these areas and an extensive rehabilitation program is needed to minimize the likelihood of recurrent injuries. The repetitive and tedious nature of such exercises, therefore, makes robotic devices an attractive alternative to manual manipulation. In fact, robots can play an important role in improving the rehabilitation outcomes in number of ways [15]. Physical efforts of therapists, with the aid of robots, can be reduced to a large extent. Moreover, sensor data related to the treatment can be collected and processed into useful information to help therapist in evaluating and treating injuries more objectively [16]. However, large variability observed between different patients due to either their level of injury or their ankle characteristics such as joint limits and stiffness also means that any robotic device employed in this area must be adaptive to allow it to cater for the requirements of specific patients.

Consequently, robots have been developed for ankle rehabilitation and most of the initial endeavors are serial robots developed to be used during gait trainings [17]–[21]. Ankle rehabilitation robot can be classified into two categories in terms of its use and the mobility of the device during operation such as exoskeletons and robotic platforms. Ankle rehabilitation exoskeletons are typical robotic orthosis used to correct the user's gait pattern [17]–[21]. Robotic platforms on the other hand, manipulate the user's foot using their end effectors and are generally developed to facilitate the treatment of ankle sprains [22]–[26]. Robotic platforms are used while sitting whereas exoskeletons are used while walking.

In this research, only sprained ankle treatment has been considered and therefore, devices used for gait rehabilitation for neurological disorders have not been discussed. It has been found that owing to their high stiffness and larger payload capacity parallel robots are better candidates for ankle rehabilitation, [27]. As a result, few parallel robots have been developed for ankle sprain rehabilitation. In one of the earliest works in this direction, Girone *et al*. proposed the *Rutgers Ankle* that used a Stewart platform, capable of providing 6 degrees of freedom (DOF) to the ankle joint [22]. Although the Rutgers Ankle has been developed and is being used for scientific experiments, its redundant actuation is a serious drawback. The position of the ankle joint in the robot does not remain stationary, causing inconvenience to patients and difficulty in designing a suitable controller. In order to reduce the redundancy of the aforesaid Stewart platform, Later, Dai *et al*. [28], [29] proposed a parallel robot for sprained ankle treatments employing less DOF. Another instance of parallel robot used for ankle joint rehabilitation is found in [30] where a single platform-based reconfigurable robot mechanism has been proposed. Another 3-RSS/S parallel mechanism is proposed by Liu *et al*. [31] and the kinematic design of its prototype is validated using only simulations. Lately, Syrseloudis and Emiris [25] have proposed a tripod-based parallel robot actuated by electric motors.

All these ankle robots have similar structure wherein the patient is required to place their foot on top of a foot platform, actuated from the bottom. These robots employ heavy linear motors for actuators and have a fixed base which means that they are not portable. Apart from having fixed base there are certain other pragmatic issues with this configuration such as noncompliant actuations, slip between robot and human foot, and higher costs. First, when the robot foot platform, containing the patient's foot, is moved, position of the ankle joint and the shinbone keeps changing with respect to the ground [see Fig. 1(a)]. This instability in the position of the ankle joint leads to control errors that are difficult to comprehend and cause discomfort to the patient. Second, due to use of bulky actuators and overall heavy robot structure, a significant slip between robot and subject's foot is anticipated and therefore the robot shall not remain compatible to foot during ankle motions [32]. To overcome the aforementioned limitations of existing ankle robots, a new parallel robot has been developed by the authors (see Fig. 2). The newly developed ankle robot design has actuators placed parallel to the shinbone [see Fig. 1(b)] of the subject and therefore position of the ankle joint and the shinbone remains unaltered during treatment. The new ankle robot is light in weight and remains compatible with the ankle motions since it uses inherently compliant pneumatic muscle actuators (PMA) that are also quite light in weight. Evaluation of this new design has been performed during present research to assess its feasibility in ankle rehabilitation. A fuzzy logic-based approach, to control ankle robot and realize rehabilitation treatment, has also been proposed. In order to evaluate performance of this controller, experiments with a neurologically intact subject were carried out and the results were analyzed.

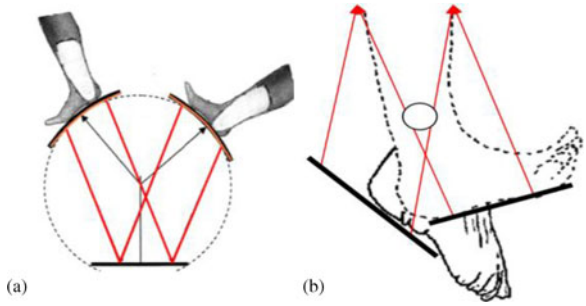

Fig. 1. (a) Varying foot and ankle positions in platform type parallel robots. (b) Anatomically correct arrangement of actuators to maintain ankle joint stationary. Red lines represent actuators.

II. Methodology

A. Ankle Robot Design Description and Analysis

For the purpose of designing a cost-effective, safe, compliant, and wearable solution for an ankle joint rehabilitation robot, the ankle complex motions were studied (see Table I). The requirements in terms of ROM and force exerting capabilities at the ankle joint formed the basis of the proposed ankle robot design. Subsequently, various concepts were perceived and analyzed for their feasibility. A design which is finally chosen is shown in Fig. 2. This robot design is able to provide three rotational degrees of freedom to the ankle joint for the necessary ROM and muscle strengthening exercises [33]. It employs

This article has been accepted for inclusion in a future issue of this journal. Content is final as presented, with the exception of pagination.

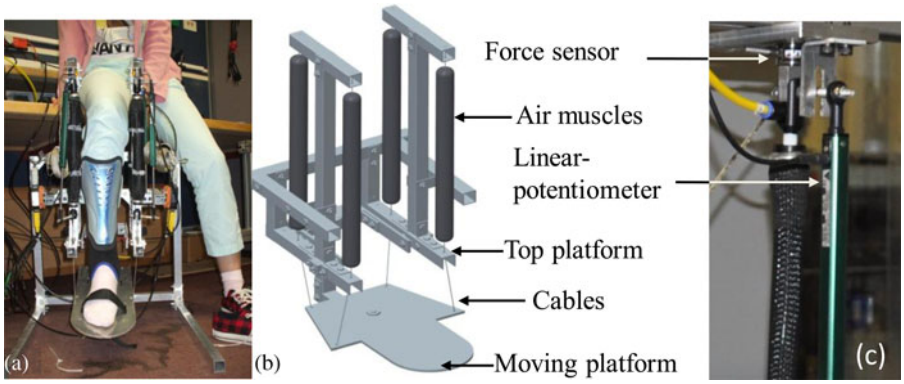

Fig. 2. Wearable ankle robot while in use (a) Robot in use after construction. (b) 3-D solid model of the final concept. (c) Positions of force sensors and linear potentiometers.

TABLE I
TYPICAL ROM AT THE HUMAN ANKLE AND CORRESPONDING ROBOT CAPABILITIES

Type of motion	Required Range	Robot capabilities: Maximum motion	Robot capabilities: Moment capacity
Dorsiflexion	20.3°- 29.8°	46°	120Nm
Plantarflexion	37.6°- 45.75°	46°	120Nm
Inversion	14.5°- 22°	26°	96Nm
Eversion	10°- 17°	26°	96Nm
Adduction	22°- 36°	52°	68Nm
Abduction	15.4°- 25.9°	52°	68Nm

Data reproduced from [1].

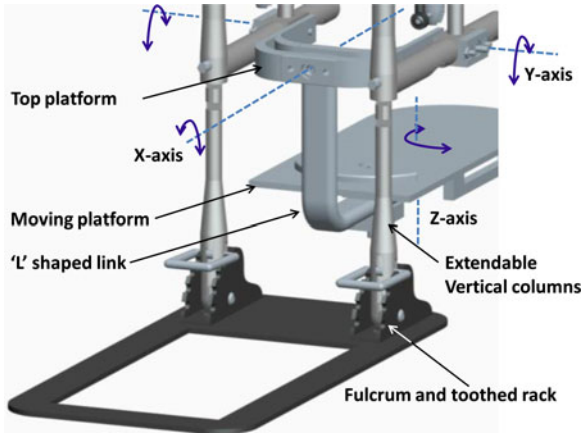

Fig. 3. Details of the ankle robot mechanism and motions.

two parallel platforms; a "U" shaped top platform (TP) built-in with a leg support structure and a moving platform (MP) at the bottom, designed to accommodate the foot and the ankle of patients. PMA [34] are employed with their actuating ends connected to the MP through flexible steel cables. Use of flexible cables along with PMA helps in achieving kinematic compatibility [35]. The MP is connected with the robot structure via "L"-shaped link, which has two bearings one at the base and the other on the vertical surface. This link provides 2-DOF (inversion–eversion and adduction–abduction) to the MP while the third DOF (dorsiflexion–plantarflexion about the y-axis) of the link and MP combine is achieved through two bearings mounted on the TP as shown in Fig. 3. Dimensions of MP and other robot parts are carefully selected so that the required ROM can be achieved. As can be seen from Table I, the achievable workspace of the ankle robot matches to the actual ankle motion requirements.

Ankle joint has high stiffness [36] and therefore the use of parallel kinematic structure for ankle robot can be justified since they have higher stiffness to avoid possible deformations and associated positional errors. Considering available forces from the actuators and their connection points on both the platforms, the overall moment exerted by the actuators at the MP can be calculated. Moment capacities of the ankle robot shown in Table I are also found to be sufficient in carrying out muscle strengthening exercises at ankle joint [37]. The robot design is right–left symmetric so that the left or right foot-ankle joints can be treated using the same robot. Moreover, its design features are adaptable to subjects of different physical abilities and age groups. Two vertical columns (see Fig. 3), which are holding the mechanism upright, have been designed to be extendable to adapt to varying shank lengths of subjects. The robot can be adapted to the patient's sitting posture by tilted it desirably and moving the whole assembly about the fulcrum on a toothed rack as shown in Fig. 3. Length and width of the rectangular MP is adjustable and varies between 200–300 mm and 80–120 mm,respectively. Certain requirements, which come from the wearable aspect of the robot, have also been considered in the proposed design. These are portability, compact size, lightweight (the ankle robot weighs less than 3 kg), friendly appearance, ease to put on and remove, etc. Using PMA, the robot is expected to have low impedance to allow backdrivability which will further help the robot in minimizing trajectory errors during assistive motions [18], [38].

PMA are chosen due to their very lightweight and compliant action. These actuators can deliver power-to-weight ratio as high as 400:1 compared to the pneumatic cylinders and dc motors that can deliver only 16 times of their weight [39]. The actuation of PMA, in general, can be characterized equivalent to the human skeletal muscles. Weight of a 30-cm-long PMA is 80 gm

This article has been accepted for inclusion in a future issue of this journal. Content is final as presented, with the exception of pagination.

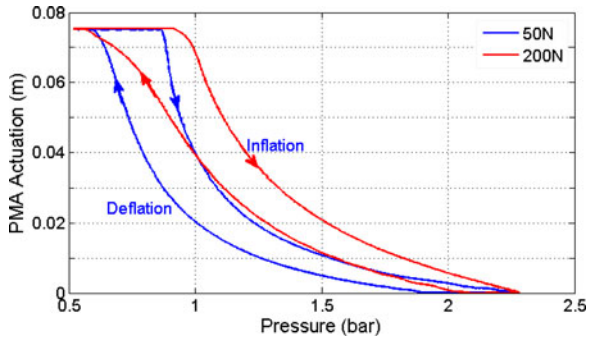

Fig. 4. Characteristics of PMA at different loads.

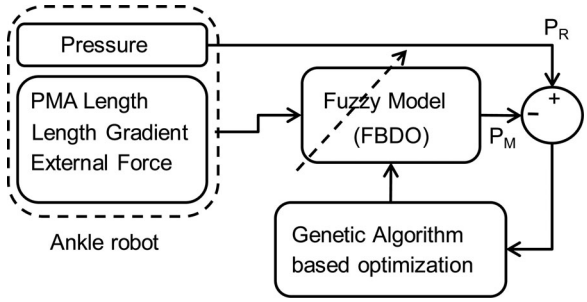

Fig. 5. System identification of FBDO using genetic algorithms.

and it can exert more than 700-N pull force when operated at 4-bar pressure [40]. A pressurized air supply is given to the four PMAs through pneumatic control valves for their sequential and simultaneous actuation.

It is known that robots using cables along with actuators will lose controllability if during operations one of the cables becomes slack or is not in tension [41]. Thus, it is important to ensure that all the cables remain under tension during robot motions. Further since the PMA can only pull and cannot push, to maintain the tension in all the cables during operations, it is important to have redundant actuation. In fact, redundant actuation is a prerequisite for all the cable-based parallel robots that means that "$(n+1)$" actuators are required to achieve "n"-DOF motion of the manipulator [41]. Therefore, in the aforesaid prototype, four sets of PMA in series with cables are used to obtain 3-DOF from the robot. Coordinated and antagonistic actuations of PMA will ensure the desired changes in the cable lengths to achieve a required pose of the MP for a range of ankle exercises. Ankle robot employs three types of sensors, namely, linear potentiometers, load cells, and pressure transducers to measure position, force, and pressure inside PMA, respectively. Load cells have been connected in series with the PMA, whereas linear potentiometers are connected parallel to the actuator. Pressure transducers have been attached to the pneumatic supply line close to the actuators in order to avoid measurements errors due to losses in the line.

Safety: Several safety features were incorporated in the ankle robot design and control hardware. Mechanical stops were placed on the joints to avoid the MP to go beyond the physiological ranges of motion. These mechanical stops can withstand the maximum torques applied by the PMA. Two emergency switches were wired such that, a single push can stop the whole system. One switch button was held by the subject while the other was held the person invigilating the training process.

B. Actuator Modeling

Although PMAs have many advantages over other actuators, their nonlinear and time-dependent behavior is a matter of concern [42]. Characteristics of PMA obtained during our experiments at The University of Auckland are shown in Fig. 4. This illustration provides at least three important information regarding PMA behavior. While the actuation varies nonlinearly with the pressure it also depends whether PMA is being inflated or deflated. In other words, different PMA characteristics are obtained when PMA are inflated and deflated. Furthermore, the PMA behavior is also sensitive for the external load acting on it. As seen in the same illustration (see Fig. 4), the characteristics shifts rightwards when external load on PMA is increased discretely from 50 to 200 N. Existing methods to model the static and dynamic behavior of PMA are studied during this research and it is found that in almost all the previous research work, PMA were modeled for fixed loads without considering the effect of external load variation [34], [43]–[47]. However, in the present application the external force on the robot due to its interaction with human user is expected to change continuously. Therefore, authors previously had developed a fuzzy-based disturbance observer (FBDO) for PMA that provides accurate pressure values by compensating the effects of external load variations [45]. A *Takagi–Sugeno–Kang (TSK) inference*-based fuzzy system [48] is adapted in designing the FBDO.

Inputs to the FBDO are PMA length, gradient of this length with respect to time and the external force on PMA whereas output from the observer is the pressure inside PMA. Length, force, and pressure information was obtained using sensors as shown in Fig. 2 on the ankle robot. Verily, the knowledge base and the rule base of fuzzy system are required to be optimized for enhanced accuracy of the disturbance observer [49]. Genetic algorithm was used to obtain the parameters of fuzzy system by minimizing error between the pressure measured through sensors mounted on the robot P_R and the pressure obtained from FBDO P_M as system output [45]. The optimization of FBDO has been schematically shown in Fig. 5. Details of FBDO and its optimization have been discussed in [45] and are recommended for further reading.

C. Adaptive Fuzzy Logic Controller

The wearable ankle robot is intended to perform ROM and muscle strengthening exercises. This requirement can be achieved by controlling lengths of the four actuators and bringing the MP in a required orientation or pose. Since the MP pose is acquired by the coupled motion of its actuators, inverse kinematics relation (1) can be used to find the required link vector comprising of actuator lengths to achieve a desired MP pose

$$L_i^o = (P_e^o + R_e^o a_i^m - b_i^f). \tag{1}$$

This article has been accepted for inclusion in a future issue of this journal. Content is final as presented, with the exception of pagination.

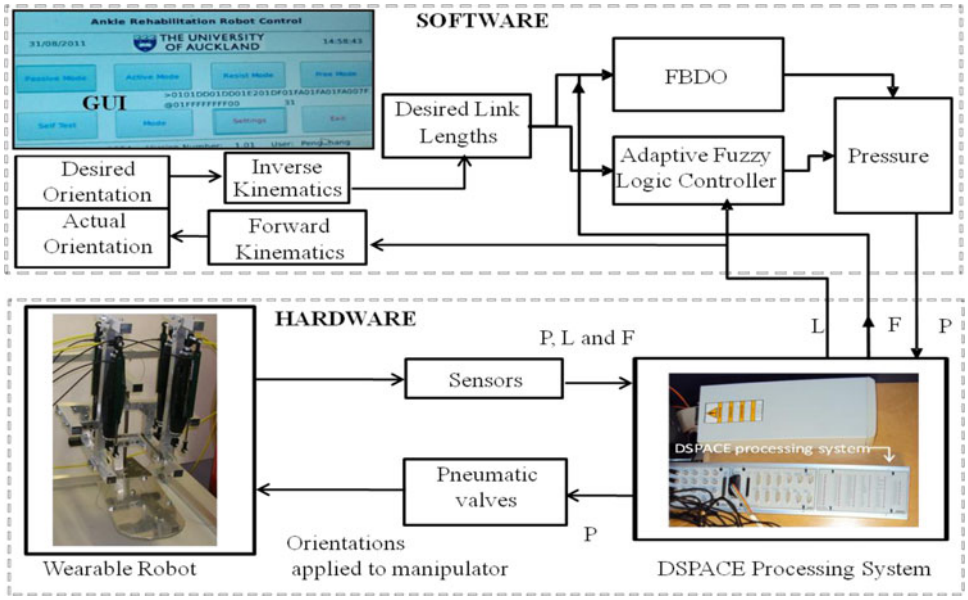

Fig. 6. System configuration of the wearable robot.

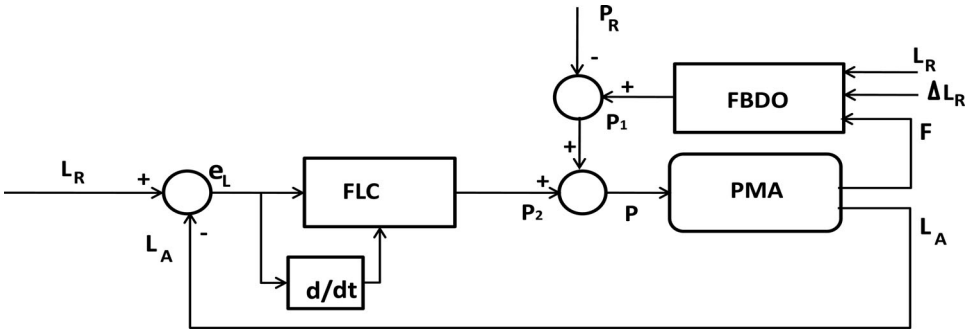

Fig. 7. Overall fuzzy control scheme used for the wearable robot.

Here, L_i^o gives instantaneous actuator length, P_e^o is the location of ankle joint, R_e^o is the standard rotational transformation matrix, and a_i^m and b_i^f are the coordinates of connection points at the MP and TP, respectively. The inverse kinematics and forward kinematics (FK) analysis of the proposed robot have been discussed elsewhere in our previous work [50] and the same can be referred for further details. It is important to note that in the present case a controller working on inverse kinematics scheme cannot be accurate owing to PMA's nonlinear behavior. The characteristics of PMA are also sensitive to the unmodeled external dynamics. During operations, actuators of the parallel ankle robot experience different forces that further mean that the orientations of the MP will be achieved with different link velocities. Some of the actuators may behave sluggishly when the external force on them is large and eventually take more time to achieve a target pose. Since the simultaneous actuation of four PMA results in the desired MP orientations, different velocities of individual actuators results in the orientation errors along with accumulated trajectory following errors. Moreover, to realize muscle strengthening exercises on the robot, a force control strategy needs to be implemented that can only be achieved by controlling pressure in the actuator.

In the light of earlier discussion, it can be concluded that the inverse kinematics approach, wherein the actuator lengths are controlled, cannot be used in the present case. Hence, pressure was considered as a control variable and actuator lengths were controlled by inflating or deflating them in order to achieve required MP orientations. A control scheme based on an open-loop feed-forward controller cannot be considered as stable [51]. Moreover, rehabilitation applications, involving human user, have higher safety requisites [15], thus a closed-loop feedback controller is preferred over an open-loop controller. Conventional controllers, such as variants of proportional-integral-derivative controllers, work well only with linear and predictable system. Incorporating parametric modifications and system identification mechanisms, conventional controllers can control nonlinear systems. However, systems which are nonlinear and have inherent uncertainty cannot be controlled using conventional controllers [49], [52]. Human–robot interaction control is an instance of such system, which is highly nonlinear and has uncertain dynamics that are impossible to model [35]. Fuzzy logic controllers (FLC), on the other hand, have proven their usefulness in the realm of uncertainty and ambiguity and hence a FLC based on Mamdani inference was

This article has been accepted for inclusion in a future issue of this journal. Content is final as presented, with the exception of pagination.

TABLE II
FUZZIFICATION OF THE ANTECEDENT AND CONSEQUENT FUZZY VARIABLES USED IN THE ADAPTIVE FUZZY CONTROLLER

	Linguistics / Activation	NB	NS	ZE	PS	PB
Pressure (bar)	1	-3.0	-1.5	0.0	1.5	3.0
	0.5	-2.0	-2.25, -0.75	-0.75, 0.75	0.75, 2.25	2.25
	0	-1.0	-3.0,0	-2.0,2.0	0.0,3.0	1.0
Error in Length (m)	1	-0.025	-0.0125	0.0	0.0125	0.025
	0.5	-0.0175	-0.0175, -0.005	±0.005	0.0075, 0.0175	0.0175
	0	-0.01	-0.025,0.0	±0.015	0.0,0.025	0.01
Gradient of Error (m)	1	-0.005	-0.0025	0.0	0.0025	0.005
	0.5	-0.004	-0.004, -0.001	±0.001	0.001, 0.004	0.004
	0	-0.002	-0.005,0	±0.003	0,0.005	0.001

developed for the present application [52], [53]. The overall system configuration and control scheme, which incorporates the FBDO, FLC, GUI, and hardware, have been shown in Figs. 6 and 7. The FLC takes two inputs which are error in actuator length and the gradient of this error. Output from the FLC is pressure (bar), which is later converted to duty cycles using pulsewidth modulation (PWM).

The FBDO and FLC were implemented in Simulink, which is the control platform used in MATLAB. The desired orientations of the MP were converted into sets of link lengths using the inverse kinematics module (1). The vector of required link lengths along with force sensor readings was given to the FBDO. Similarly, the desired link lengths and the vector of actual link lengths, obtained from the linear potentiometers, was given to the FLC as inputs. Output from both, the FBDO and FLC, was pressure which was aggregated and converted in terms of duty cycles (using PWM) to be provided to the individual pressure valves. This information was passed onto the valves through the DSPACE processing system. Pressure values obtained from the controller was applied to the individual PMA of ankle robot and the required orientation of the MP was achieved. Observations from the sensors for position, force, and pressure were read through DSPACE system. Force information was used by the FBDO, whereas position information was shared by FLC and the FK module [50]. Actuator length information was converted to MP pose using FK module and this information was used to find the error in the MP orientations. Fuzzification of antecedent and consequents variables of FLC, development of the rule base and the inference mechanism used to calculate required pressure values, have been explained in the next section.

Antecedent and consequent modeling: Fuzzification is an important step in design of a fuzzy controller. During this process, the antecedents and the consequents are converted into fuzzy variables. Five Gaussian activation functions (AFs), linguistically defined as negative big (NB), negative small (NS), zero , positive small (PS), and positive big (PB) are used to represent each of the inputs ($\boldsymbol{e}$ and $\boldsymbol{\Delta e}$) and output ($\boldsymbol{P}$) fuzzy variables (see Table II). Higher number of AFs was chosen to ensure better discrimination while predicting pressure values. In order to design a fuzzy system, its parameters are required to be defined.

TABLE III
RULE-BASE TABLE USED IN FLC2 TO DETERMINE FUZZY PRESSURE VALUES

P		**e**				
		NB	**NS**	**ZE**	**PS**	**PB**
Δe	**PB**	**ZE**	**PS**	**PB**	**PB**	**PB**
	PS	**NS**	**ZE**	**PS**	**PB**	**PB**
	ZE	**NB**	**NS**	**ZE**	**PS**	**PB**
	NS	**NB**	**NB**	**NS**	**ZE**	**PS**
	NB	**NB**	**NB**	**NB**	**NS**	**ZE**

The knowledge base of the fuzzy systems consists of position and spread of the AFs [49]. Similarly, the rule base is a set of rules that connects input and output variables of the system using *if–then* statements as explained in the next section. AFs (such as, NB, NS, etc.) require two variables for their definition, which are their mean and standard deviation. Therefore, while developing FLC, a total of 30 parameters were needed to define a total of 15 AFs (10 for the two antecedents ($\boldsymbol{e}$ and $\boldsymbol{\Delta e}$) and 5 for the consequent ($\boldsymbol{P}$) variable). These parameters were chosen by equally dividing the universe of discourse of individual variables to accommodate all the AFs [53].

Rule-base construction: Rule base is the kernel of a fuzzy controller and it connects antecedents and consequents using an *if–then* relationship. An instance of the fuzzy rule is given next

$$\overbrace{\text{if } e \text{ is } A_{i1} \text{ and } \Delta e \text{ is } A_{i2}}^{\text{Antecedents}} \overbrace{\text{then } P \text{ is } B_i}^{\text{Consequents}}.$$

Total number of rules for a fuzzy controller can be given by the following relation:

$$N_r = \Pi_{k=1}^{N} m_k \tag{2}$$

where N_r represents the total number of rules, N is number of input variables, and m_k is the number of linguistic terms of kth input variable. Since there are two input variables represented by five AFs each in the present case, the total number of rules is 5^2, i.e., 25 (see Table III). Rule base for the FLC has been

This article has been accepted for inclusion in a future issue of this journal. Content is final as presented, with the exception of pagination.

developed by analyzing and inferring the experimental findings. An inference mechanism later aggregates all individual rule outputs and provides the final pressure value for given inputs. Three kinds of inference mechanisms were proposed in the literature namely, Zadeh max–min inference, Mamdani min–max inference, and Larson product inference [52]. Out of these the Mamdani min–max inference has been selected. which is more popular owing to its simplicity in software and hardware implementations [53]. Various steps, while implementing the Mamdani inference in this study, have been explained later.

Initially, the crisp set of input variables (e and Δe), obtained from robot sensors, was converted into fuzzy variables. The operator "*min*" was applied on these two fuzzy variables to compute the fuzzy value of the consequent variable P for all the rules. Subsequently, outputs from all the rules were aggregated and then defuzzified to provide a crisp output value. This process is explained using the following equations (3)–(6). The inference result $\mu_{\mathrm{Bi}}(P)$ for a certain rule was computed applying a "*min*" operator on the input values as shown

$$\mu_{\mathrm{Bi}}(P) = \mu_{A_1 i}(e) \wedge \mu_{A_3 i}(\Delta e) \wedge \mu_{\mathrm{Bi}}(P). \tag{3}$$

Here, $\wedge$ stands for "*min*" and $\mu_{A_1 i}$, etc., are the activation values for the individual input variables in ith rule. The final value of the fuzzy consequent variable was found by applying a "*max*" operator to the individual rule outputs as shown in (3)

$$\mu_B(P) = \mu_{\grave{B}1}(P) \vee \ldots \vee \mu_{\grave{B}N_r}(P). \tag{4}$$

Here, $\vee$ stands for "*max*". The pressure value so obtained is a fuzzy variable and hence cannot be used in real-time application unless converted into a crisp real number. The process of translating fuzzy variables into real numbers is opposite to the *fuzzification* process and hence termed as *defuzzification*. There exist several *defuzzification* methods proposed by researchers and these methods can be broadly classified as methods based on the geometry of the fuzzy set [54] and methods using statistical interpretations [55]. Among these the centroid or the centre of gravity method is often used due to its simplicity and easy hardware implementation. Centroid method was used in this study to convert the fuzzy output P in a usable crisp form P_0 as explained in

$$P_0 = \frac{\int P \mu_{\acute{B}}(P) dP}{\int \mu_{\acute{B}}(P) dP}. \tag{5}$$

To avoid the complex computation involved in evaluating aforementioned integral a simplified form was used here

$$P_0 = \frac{\sum_{i=1}^{N_r} P_i \mu(P_i)}{\sum_{i=1}^{N_r} \mu(P_i)}. \tag{6}$$

Here, P_0 is the crisp output for pressure from the model, P_i are the fuzzy outputs from individual rules, and $\mu(P_i)$ represent their activation values.

Adaptive mechanism: It was found from the experiments that to attain a certain length of PMA, comparatively less pressure is required during deflation cycle (see Fig. 4). Therefore, depending on whether the position gradient of PMA is positive or negative, the amount of pressure requirement, for attaining a certain position, is different. This time-dependent behavior, shown by the PMA, can be attributed to the hysteresis phenomenon present in the latex tube, which is used as its inner core. The hysteresis effect (see Fig. 4), present in PMA, is due to the changed strain-energy density of the latex tube. Bertetto and Ruggiu and others [56], [57] had earlier investigated this effect and had proposed the nonlinear Mooney–Rivlin model to account for the hysteresis in PMA.

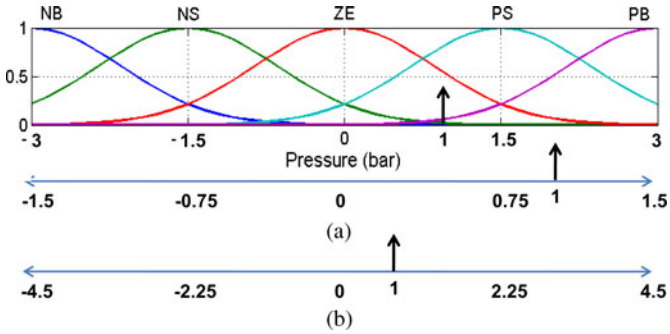

Fig. 8. Effect of using a SI on output variable's universe of discourse: (a) SI = 0.5 and (b) SI = 1.5.

Although FLC are designed to control nonlinear systems, the time-dependent characteristics are difficult to model accurately. Nevertheless, by introducing an adaptive mechanism into the controller, errors in controlling time-varying uncertainties can be reduced [58]. The controller parameters are required to be altered to improve controller performance as and when the course of PMA actuation changes. While adaptive fuzzy controllers have been researched in the past and few adaptive schemes have been proposed in the literature, they all are limited to the theoretical analysis [58]–[61]. Conversely, in this study an adaptation mechanism has been implemented in the real time that dynamically changes the universe of discourse of the output pressure variable.

As shown in Fig. 8, the fuzzy set definition changes significantly when different scaling indices are applied. A pressure value of 1 bar which was between ZE and PS (linguistic description) becomes close to PB when a scaling index (SI) of 0.5 is applied. Similarly applying a SI of 1.5, it changes to close to 0. Thus, by changing SI the sensitivity of the controller can be altered. In this case, the SI is obtained from the gradient of actuator length with respect to time and varies linearly between 1.0 and 1.4 with the gradient values (6)

$$\mathrm{SI} = -40 \times \mathrm{grad}(L) + 1.2. \tag{7}$$

The aforesaid empirical relation has been obtained through the analysis of experimental findings. There are two valid reasons for using this adaptive scheme, first, users with different physical capabilities will be using this device and thus different forces will be applied on individual actuators leading to anomalies in actuator actuations. Second, we have observed that over the time and with use, actuator lengths also change (a slight increase in actuator length is observed with excessive use due to the elastic nature of their inner latex tube). Increased actuator lengths lead to a slight decrease in the actuation velocities that needs to be compensated. Increased pressure in the actuators

This article has been accepted for inclusion in a future issue of this journal. Content is final as presented, with the exception of pagination.

has been found capable of maintaining actuation velocities. Since the grad L increases with time (after excessive use), to maintain the actuation velocity the pressure inside the actuators is required to be increased. The proposed adaptation (see equation 7), however, is able to provide the increased pressure to cope with the increase in the grad L. Apparently, the gradient of length is negative during inflation (actuator length is shortening) that makes the SI positive and greater than one. Eventually, fuzzy rule outputs such as PS, PB, etc., corresponds to greater pressure values due to increased pressure scale and pressure given to the actuator will be increased. However, during deflation cycle when the gradient of length is positive, the SI still remains positive due to the positive constant (>1) in the function and its value will be close to unity, which would mean that no significant change in the pressure is required.

Thus, in the inflation cycle, increased range of pressure is applied compared to the deflation cycle. Following aforesaid empirical relation, the maximum pressure in PMA has been observed to vary between 3 and 4 bars.

III. Experimental Results

A healthy, neurologically intact subject (male, age 25 years) with no history of neurologic disorders gave written informed consent and participated in the study. Appropriate approvals for this protocol were obtained from the Human Participants Ethics Committee at The University of Auckland.

A. Experimental Protocol

The adaptive fuzzy controller appended with the FBDO was implemented on the ankle robot prototype with the aim of evaluating robot's performance in ankle rehabilitation treatments. First, experiments were performed on a single PMA while it was being loaded in the range of 50–200 N. Later, experiments with the ankle robot were investigated and to begin with, the robot was subjected to a step signal to check the response of the group of PMA in terms of maximum velocity and overall stability of the robot. During these experiments the overshoot and ringing were not observed, and thus the robot motions were considered stable for the input signal. Subsequently, experiments were carried out while the wearable ankle robot was being used by the healthy subject and controlled using the adaptive FLC. Experiments were performed with two sets of objectives. The primary goal of the trajectory tracking experiment was to validate the capability of the ankle robot to help subjects in completing the foot motions across a wide workspace even when they are severely injured. Further, these experiments and their findings are also aimed to facilitate the analysis of controller performance when the robot interacts with the unknown external environment. Motion trajectories that are normally used by the therapists namely, dorsiflexion–plantarflexion, inversion—aversion, and adduction–abduction were implemented [28], [62]. To begin with, right foot of the subject was secured in the MP of the wearable ankle robot conveniently and the user was asked to sit comfortably. The passive mode of the rehabilitation treatment was investigated wherein the subject was asked not to exert any force and remain relaxed while the robot was commanded to implement the three trajectories aforementioned. The desired orientations of the MP for the commanded trajectories were $\pm\pi/3$, $\pm\pi/6$, and $\pm 5\pi/36$ radians for the dorsiflexion–plantarflexion, inversion-aversion, and adduction–abduction motions, respectively [1].

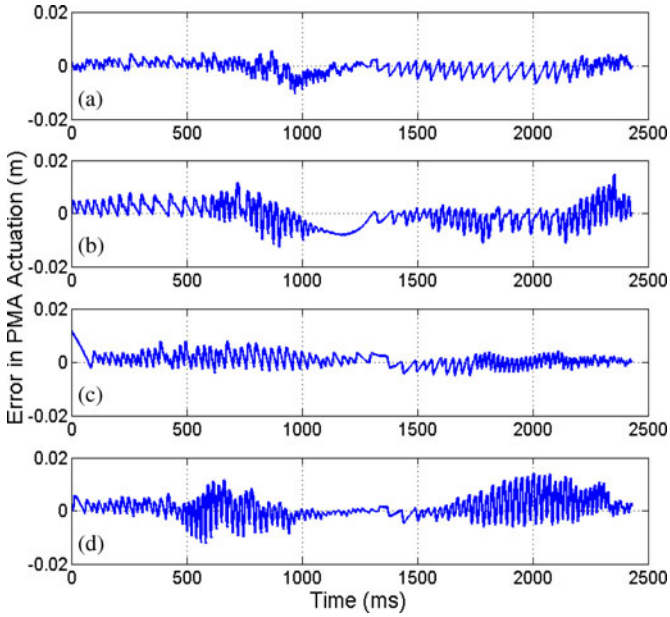

Fig. 9. Trajectory tracking errors for a single PMA at varying loads: (a) 50 N, (b) 100 N, (c) 150 N, and (d) 200 N.

B. Results

In this section, the preliminary results of the overall fuzzy controller are presented. For the purpose of analysis, a small segment representing the complete data is plotted here. To begin with, experiments were performed whereby a single PMA was attached to discretely varying loads in the range of 50–200 N. The PMA was actuated to follow a random trajectory and excellent trajectory tracking results were obtained. Trajectory tracking errors, as the PMA was subjected to different loads, have also been displayed in Fig. 9. While maximum tracking error was observed to be ± 0.015 m, the mean squared error was of the order of 10^{-5} m. Subsequent experiments involving human subject were carried out with the ankle robot. Desired actuator lengths, obtained using inverse kinematics, were plotted along with the resulting actual link length information (obtained from the linear potentiometers) for dorsiflexion–plantarflexion trajectory as shown in Fig. 10. Initially, all the actuators were at their mean position that is shown as 0.1125 m. Here, trajectories shown using dotted lines are the desired values for link lengths, whereas the actual link lengths, recorded from the sensors, are shown using solid lines. Maximum deviation in the link lengths was recorded to be 0.0240 m, whereas the standard deviation was found to be 0.0104 m. Later, using FK module, the actual MP orientations were computed and plotted for the three trajectories separately along with the desired orientations as shown in Fig. 11. Trajectory following error was also recorded and their magnitudes and the irregular pattern were analyzed. While

This article has been accepted for inclusion in a future issue of this journal. Content is final as presented, with the exception of pagination.

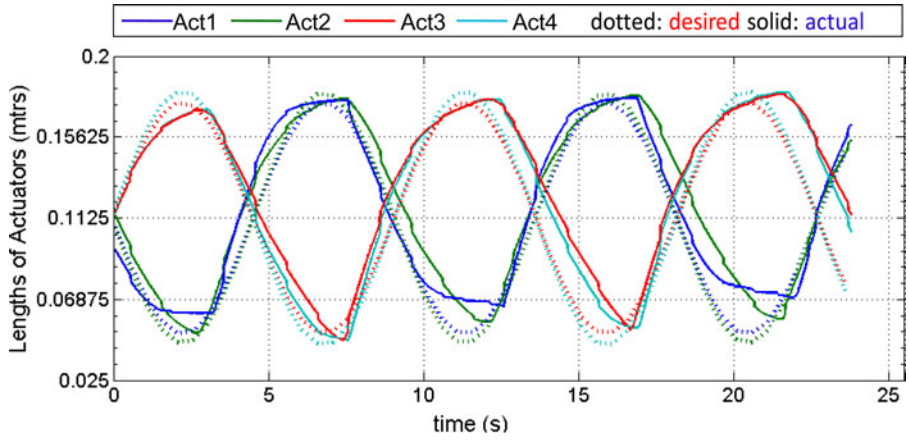

Fig. 10. Trajectory following response of individual actuators for dorsiflexion–plantarflexion trajectory while the robot is being used by a healthy subject in passive mode.

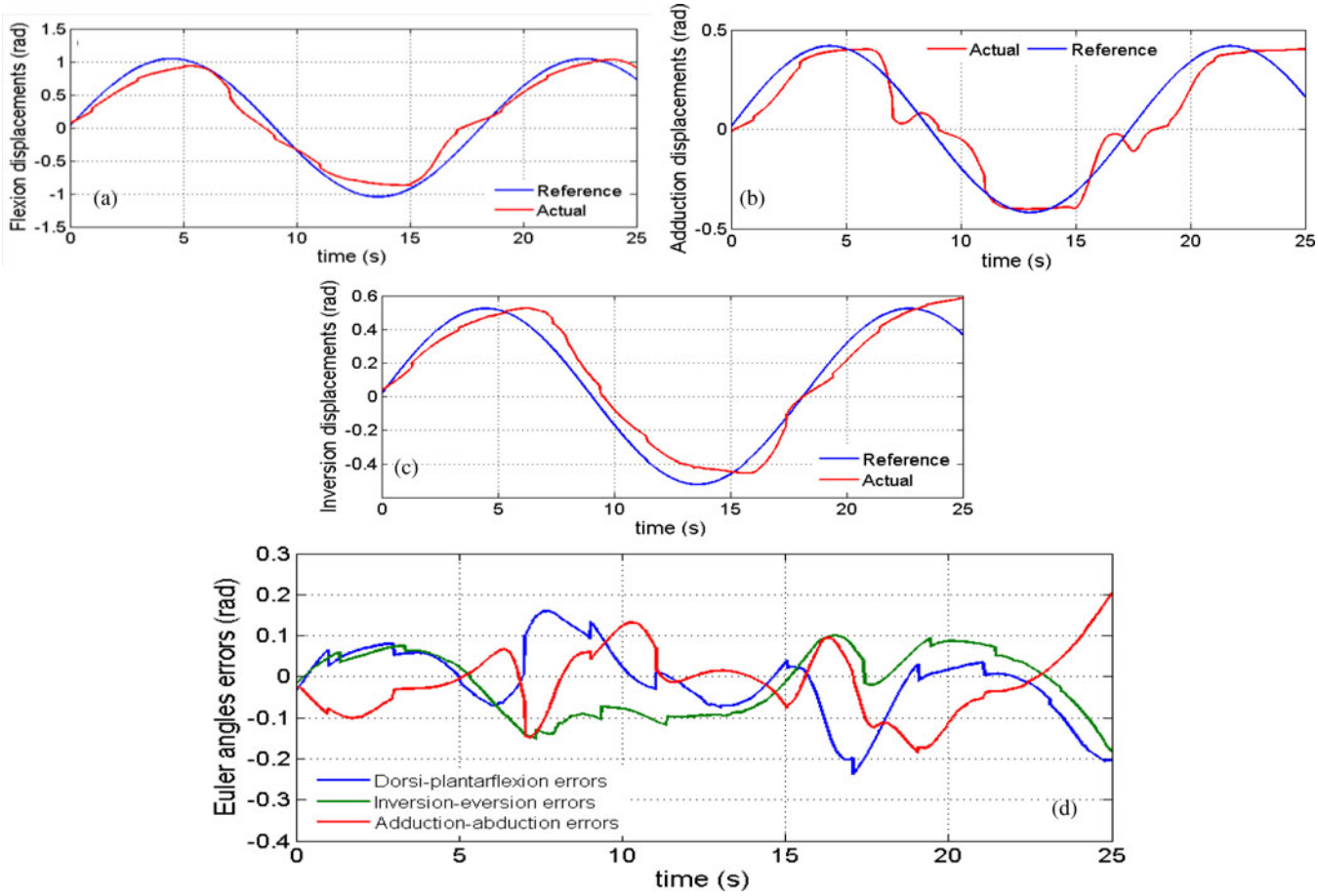

Fig. 11. Trajectory following response in Euler angles for three types of trajectories, namely, (a) dorsiflexion–plantarflexion, (b) Adduction–abduction, and (c) inversion–aversion; and trajectory following errors, (d) while the robot is being used by a healthy subject in passive mode.

the absolute mean error recorded from these experiments was 0.086 rad, the maximum error was found to be 0.2 rad. The maximum velocity of the robot motion was found to be approximately 0.0417 m/s, which is taken as acceptable given the slow motion requirement during rehabilitation treatments.

IV. Discussion and Conclusion

Ankle sprains are the common forms of musculoskeletal injuries and an extensive rehabilitation program is typically required to reinstate ankle functions and avoid reinjuries.

This article has been accepted for inclusion in a future issue of this journal. Content is final as presented, with the exception of pagination.

Therefore, in order to extend adequate therapy to the patients, various robotic platforms have been developed for the ankle joint rehabilitation. These robots are expected to reduce the physical workload of therapists and supplement the resources required to facilitate a comprehensive rehabilitation program.

It was revealed after a careful survey of the literature that existing robots are undesirably inspired by industrial robot designs and therefore have problems. Problems with existing ankle robot have already been discussed in Section I. Some of the shortcomings that are common to all these contemporary robots are, incompatibility with the ankle joint during motions, stiff actuation, nonbackdrivability, high cost, unfriendly or intimidating appearance due to use of heavy and bulky electromagnetic actuators. Moreover, as significant variability can be present in terms of joint characteristics and severity of impairment between different patients, further development is still required to enhance the adaptability of such robotic systems.

This research addresses the aforementioned issues through the development of a novel ankle rehabilitation robot that can be adapted to different users with minimal hardware or software modifications. The proposed ankle robot can be directly attached to the shinbone of the subject and due to better placement of actuators; the robot remains compatible to the ankle joint during various motions. The proposed ankle robot has biologically inspired design, compliant actuation and therefore it is backdrivable and safe to use. Design capability of the proposed design has been analyzed and it was found that the robot is capable of providing 3-DOF to the ankle joint with requisite moments (see Table I). Safety provisions are vital and proper care has been taken to stop the robot actuation when desired and bring the MP back to its initial configuration quickly. To achieve compliant motion and reduce the overall weight of the ankle robot, PMAs have been used in place of linear electrical motors. PMAs are powerful actuators and have characteristics that are similar to the skeletal muscles. However, owing to their nonlinear and transient nature, PMAs are difficult to model. Therefore a FBDO has been designed to model the nonlinear behavior of PMA, whereas an adaptive scheme has been implemented to account for their transient nature.

It was observed that while FBDO was able to compensate for the nonlinearity of PMA and the external disturbance (friction, etc.), the transient nature of PMA could only be controlled by introducing some adaptive mechanism in the controller. A closed-loop adaptive fuzzy controller was therefore designed and implemented. The PMA behave differently during inflation and deflation cycles and it was noted that to attain a certain length of PMA, comparatively less pressure is required during deflation cycle. Consequently, a significant hysteresis is observed during the PMA actuation. The controller parameters are required to be altered to adapt to the changing course of PMA actuation. Therefore, in this study, an adaptation mechanism has been implemented that dynamically changes the universe of discourse of the output-pressure variable in accordance with the PMA actuation. To begin with, the adaptive FLC in conjunction with the FBDO was implemented to control a single actuator. Following a set of experiments, excellent trajectory tracking performance was observed (maximum tracking error ± 0.015 m, mean squared error of the order of 10^{-5}m). During these experiments, the PMA was exerted upon by loads varying discretely between 50 and 200 N. These observations were encouraging since the accuracies in trajectory tracking was 100 times better than the previously reported best results [63].

Subsequently, a control scheme for the complete ankle robot was devised as shown in Fig. 6. The ankle robot control was a challenging task due to its parallel robot-based design, use of PMA for actuators and the rehabilitation application wherein robot is required to interact with human subject. It was also found that an inverse kinematic-based approach for the robot position control was not sufficient and can lead to significant orientation errors.

While performing experiments with healthy subject, the user was asked not to exert any force and remain relaxed while the robot was commanded to implement the motion trajectories. Though the robot was able to follow motion trajectories, incoherent tracking errors were recorded due to interaction of the ankle robot with a human user. These are desired and acceptable results, since the robot is not forcing subject's ankle joint to strictly follow a given trajectory, rather a variation is allowed suiting to subject's own ankle motions. These results also show that the robot is able to provide compliant motions without much compromise in the tracking accuracy. Previously, trajectory tracking results for a serial robot employing PMA have been provided by Lilly and Quesada [42] wherein an error of the order of 0.2 radians has been reported. It is important to note that the trajectory following error reported by Lilly and Quesada [42] has been obtained during computer simulations. Conversely, in this study we have been able to achieve similar accuracy from laboratory experiments using PMA in a parallel robot and working with a human subject. Involuntary application of force by the subject on wearable robot is difficult to assess, which is a predominant source of trajectory deviations.

It is important to note here that present experiments were carried out to evaluate the ankle robot design, use of PMA and the controller performance while the robot is being used by a healthy subject. The error due to human intervention is desirable and this further strengthens our argument that the actuators are backdrivable and are allowing the patient to divert from the commanded trajectories. Since the subjects using this robot shall have inconsistent musculoskeletal properties, a compliant device is required to allow deviations and more naturalistic motions. The *variable compliance* property of the ankle robot shall be constructively utilized in future while implementing various rehabilitation strategies on the ankle robot [34].

According to the best knowledge of authors, real-time application of a novel adaptive fuzzy controller is being proposed for the first time. Moreover, application of this controller in a parallel ankle robot, actuated by inherently compliant PMA, is also a novel work wherein four PMAs have been controlled to achieve the required pose of the robot in the presence of unknown external forces. Further extension of the present research shall be in realizing various rehabilitation strategies on the ankle robot. It will be interesting to see how fuzzy logic can be used in developing advanced control strategies. Experiments with a larger

This article has been accepted for inclusion in a future issue of this journal. Content is final as presented, with the exception of pagination.

segment of subjects are also proposed to statistically study the human–robot interaction.

REFERENCES

[1] S. Siegler, J. Chen, and C.D. Schneck, "The three-dimensional kinematics and flexibility characteristics of the human ankle and subtalar joints-Part I: Kinematics," *J. Biomech. Eng.*, vol. 110, pp. 364–373, 1988.

[2] M. Dettwyler, A. Stacoff, I. A. Kramers-De Quervain, and E. Stüssi, "Modelling of the ankle joint complex. Reflections with regards to ankle prostheses," *Foot Ankle Surg.*, vol. 10, pp. 109–119, 2004.

[3] J. Hertel, "Functional anatomy, pathomechanics, and pathophysiology of lateral ankle instability," *J. Athletic Training*, vol. 37, pp. 364–375, 2002.

[4] M. R. Safran, J. E. Zachazewski, R. S. Benedetti, A. R. Bartolozzi III, and R. Mandelbaum, "Lateral ankle sprains: A comprehensive review Part 2: Treatment and rehabilitation with an emphasis on the athlete," *Med. Sci. Sports Exercise*, vol. 31, pp. S438–S447, 1999.

[5] S. Itay, A. Ganel, H. Horoszowski, and I. Farine, "Clinical and functional status following lateral ankle sprains: Follow-up of 90 young adults treated conservatively," *Orthop. Rev.*, vol. 11, pp. 73–76, 1982.

[6] B. L. Braun, "Effects of ankle sprain in a general clinic population 6 to 18 months after medical evaluation," *Arch. Family Med.*, vol. 8, pp. 143–148, 1999.

[7] R. A. W. Verhagen, G. Keizer, and C. N. Dijk, "Long-term follow-up of inversion trauma of the ankle," *Arch. Orthopaedic Trauma Surg.*, vol. 114, pp. 92–96, 1995.

[8] A. Anandacoomarasamy and L. Barnsley, "Long term outcomes of inversion ankle injuries," *Brit. J. Sports Med.*, vol. 39, e14, pp. 1–4, 2005. 10.1136/bjsm.2004.011676.

[9] M. S. Yeung, K. M. Chan, C. H. So, and W. Y. Yuan, "An epidemiological survey on ankle sprain," *Brit. J. Sports Med.*, vol. 28, pp. 112–116, 1994.

[10] P. Gross and B. Marti, "Risk of degenerative ankle joint disease in volleyball players: Study of former elite athletes," *Int. J. Sports Med.*, vol. 20, pp. 58–63, 1999.

[11] V. Valderrabano, B. Hintermann, M. Horisberger, and T. S. Fung, "Ligamentous posttraumatic ankle osteoarthritis," *Amer. J. Sports Med.*, vol. 34, pp. 612–620, 2006.

[12] C. G. Mattacola and M. K. Dwyer, "Rehabilitation of the ankle after acute sprain or chronic instability," *J. Athletic Training*, vol. 37, pp. 413–429, 2002.

[13] A. A. Gopalai and S. M. N. A. Arosha Senanayake, "A wearable real-time intelligent posture corrective system using vibrotactile feedback," *IEEE/ASME Trans. Mechatron.*, vol. 16, no. 5, pp. 827–834, Oct. 2011.

[14] H. I. Krebs, J. J. Palazzolo, L. Dipietro, M. Ferraro, J. Krol, K. Rannekleiv, B. T. Volpe, and N. Hogan, "Rehabilitation robotics: Performance-based progressive robot-assisted therapy," *Auton. Robots*, vol. 15, pp. 7–20, 2003.

[15] H. I. Krebs, B. T. Volpe, M. L. Aisen, and N. Hogan, "Increasing productivity and quality of care: Robot-aided neuro-rehabilitation," *J. Rehabil. Res. Develop.*, vol. 37, pp. 639–652, 2000.

[16] S. Ueki, H. Kawasaki, S. Ito, Y. Nishimoto, M. Abe, T. Aoki, Y. Ishigure, T. Ojika, and T. Mouri, "Development of a hand-assist robot with multi-degrees-of-freedom for rehabilitation therapy," *IEEE/ASME Trans. Mechatronics*, vol. 17, no. 1, pp. 136–146, Feb. 2012.

[17] K. Bharadwaj, T. G. Sugar, J. B. Koeneman, and E. J. Koeneman, "Design of a robotic gait trainer using spring over muscle actuators for ankle stroke rehabilitation," *J. Biomech. Eng.*, vol. 127, pp. 1009–1013, 2005.

[18] J. A. Blaya and H. Herr, "Adaptive control of a variable-impedance ankle-foot orthosis to assist drop-foot gait," *IEEE Trans. Neural Syst. Rehabil. Eng.*, vol. 12, no. 1, pp. 24–31, Mar. 2004.

[19] K. E. Gordon, G. S. Sawicki, and D. P. Ferris, "Mechanical performance of artificial pneumatic muscles to power an ankle-foot orthosis," *J. Biomech.*, vol. 39, pp. 1832–1841, 2006.

[20] K. W. Hollander, R. Ilg, T. G. Sugar, and D. Herring, "An efficient robotic tendon for gait assistance," *J. Biomech. Eng.*, vol. 128, pp. 788–791, 2006.

[21] A. Roy, H. I. Krebs, D. J. Williams, C. T. Bever, L. W. Forrester, R. M. Macko, and N. Hogan, "Robot-aided neurorehabilitation: A novel robot for ankle rehabilitation," *IEEE Trans. Robot.*, vol. 25, no. 3, pp. 569–582, Jun. 2009.

[22] M. J. Girone, G. C. Burdea, and M. Bouzit, "'Rutgers ankle' orthopedic rehabilitation interface," in *Proc. Amer. Soc. Mech. Eng., Dynamic Syst. Control Division*, Nov. 14–19, 1999, vol. 67, pp. 305–312.

[23] J. Yoon, J. Ryu, and K. B. Lim, "Reconfigurable ankle rehabilitation robot for various exercises," *J. Robot. Syst.*, vol. 22, pp. S15–S33, 2006.

[24] A. C. Satici, A. Erdogan, and V. Patoglu, "Design of a reconfigurable ankle rehabilitation robot and its use for the estimation of the ankle impedance," in *Proc. IEEE Int. Conf. Rehabil. Robot.*, Jun. 2009, pp. 257–264.

[25] C. E. Syrseloudis and I. Z. Emiris, "A parallel robot for ankle rehabilitation-evaluation and its design specifications," in *Proc. 8th IEEE Int. Conf. BioInf. BioEng.*, 2008, pp. 1–6.

[26] Y. H. Tsoi and S. Q. Xie, "Design and control of a parallel robot for ankle rehabilitation," in *Proc. 15th Int. Conf. Mechatron. Mach. Vis. Practice*, 2008, pp. 515–520.

[27] R. Kurtz and V. Hayward, "Multiple-goal kinematic optimization of a parallel spherical mechanism with actuator redundancy," *IEEE Trans. Robot. Autom.*, vol. 8, no. 5, pp. 644–651, Oct. 1992.

[28] J. S. Dai, T. Zhao, and C. Nester, "Sprained ankle physiotherapy based mechanism synthesis and stiffness analysis of a robotic rehabilitation device," *Auton. Robots*, vol. 16, pp. 207–218, 2004.

[29] J. A. Saglia *et al.*, "Control strategies for ankle rehabilitation using a high performance ankle exerciser," in *Proc. IEEE Int. Conf. Robot. Autom.*, May 2010, pp. 2221–2227.

[30] J. Yoon *et al.*, "Reconfigurable ankle rehabilitation robot for various exercises," *J. Robot. Syst.*, vol. 22, pp. S15–S33, 2006.

[31] G. Liu, J. Gao, H. Yue, X. Zhang, and G. Lu, "Design and kinematics simulation of parallel robots for ankle rehabilitation," in *Proc. IEEE Int. Conf. Mechatron. Autom.*,, Jun. 2006, pp. 1109–1113.

[32] J. L. Pons, "Rehabilitation exoskeletal robotics," *IEEE Eng. Med. Biol. Mag.*, vol. 29, no. 3, pp. 57–63, May/Jun. 2010.

[33] M. Girone, G. Burdea, M. Bouzit, V. Popescu, and J. E. Deutsch, "Orthopedic rehabilitation using the "Rutgers ankle" interface," *Stud. Health Technol. and Informat.*, vol. 70, pp. 89–95, 2000.

[34] T. Noritsugu and T. Tanaka, "Application of rubber artificial muscle manipulator as a rehabilitation robot," *IEEE/ASME Trans. Mechatronics*, vol. 2, no. 4, pp. 259–267, Dec. 1997.

[35] J. L. Pons, Ed., *Wearable Robots.* Chichester, U.K.: Wiley, 2008.

[36] S. J. Rydahl and B. J. Brouwer, "Ankle stiffness and tissue compliance in stroke survivors: A validation of Myotonometer measurements," *Arch. Phys. Med. Rehabil.*, vol. 85, pp. 1631–1637, 2004.

[37] E. Kearney, L. Weiss, and R. Morier, "System identification of human ankle dynamics: Intersubject variability and intrasubject reliability," *Clin. Biomech.*, vol. 5, pp. 205–217, 1990.

[38] B. S. Kim, J. B. Song, and J. J. Park, "A serial-type dual actuator unit with planetary gear train: Basic design and applications," *IEEE/ASME Trans. Mechatronics*, vol. 15, no. 1, pp. 108–116, Feb. 2010.

[39] P. K. Jamwal, S. Xie, and K. C. Aw, "Kinematic design optimization of a parallel ankle rehabilitation robot using modified genetic algorithm," *Robot. Autom. Syst.*, vol. 57, pp. 1018–1027, 2009.

[40] Shadow 30 mm Air Muscle—Specification, Shadow Robot Co., London, U.K., 2011.

[41] M. Hassan and A. Khajepour, "Analysis of bounded cable tensions in cable-actuated parallel manipulators," *IEEE Trans. Robot.*, vol. 27, no. 5, pp. 891–900, Oct. 2011.

[42] J. H. Lilly and P. M. Quesada, "A two-input sliding-mode controller for a planar arm actuated by four pneumatic muscle groups," *IEEE Trans. Neural Syst. Rehabil. Eng.*, vol. 12, no. 3, pp. 349–359, Sep. 2004.

[43] S. W. Chan, J. H. Lilly, D. W. Repperger, and J. E. Berlin, "Fuzzy PD+I learning control for a pneumatic muscle," in *Proc. IEEE Int. Conf. Fuzzy Syst.*, May 2003, pp. 278–283.

[44] M. Doumit, A. Fahim, and M. Munro, "Analytical modeling and experimental validation of the braided pneumatic muscle," *IEEE Trans. Rob.*, vol. 25, no. 6, pp. 1282–1291, Dec. 2009.

[45] P. K. Jamwal, S. Q. Xie, S. Hussain, and K. C. Aw, "Modeling pneumatic muscle actuators: Artificial intelligence approach," *Int. J. Inf. Acquisition*, vol. 7, pp. 151–164, 2010.

[46] T. V. Minh, B. Kamers, H. Ramon, and H. Van Brussel, "A new approach to modeling hysteresis in a pneumatic artificial muscle using the Maxwell-slip model," *IEEE/ASME Trans. Mechatronics*, vol. 16, no. 1, pp. 177–186, Feb. 2011.

[47] S. Q. Xie and P. K. Jamwal, "An iterative fuzzy controller for pneumatic muscle driven rehabilitation robot," *Expert Syst. Appl.*, vol. 38, pp. 8128–8137, 2011.

[48] P. A. S. Ralston and T. L. Ward, "Fuzzy logic control of machining," *Manuf. Rev.*, vol. 3, pp. 147–154, 1990.

[49] D. K. Pratihar and N. B. Hui, "Evolution of fuzzy controllers and applications," *Stud. Comput. Intell.*, vol. 66, pp. 47–69, 2007.

[50] P. K. Jamwal, S. Q. Xie, Y. H. Tsoi, and K. C. Aw, "Forward kinematics modelling of a parallel ankle rehabilitation robot using modified fuzzy inference," *Mech. Mach. Theory*, vol. 45, pp. 1537–1554, 2010.

This article has been accepted for inclusion in a future issue of this journal. Content is final as presented, with the exception of pagination.

[51] K. Balasubramanian and K. S. Rattan, "Feedforward control of a non-linear pneumatic muscle system using fuzzy logic," in *Proc. IEEE Int. Conf. Fuzzy Syst.*, St. Louis, MO, May 2003, pp. 272–277.
[52] K. Michels, F. Klawonn, R. Kruse, and A. Nurnberger, *Fuzzy Control*. New York: Springer, 2006.
[53] D. K. Pratihar, *Soft Computing*. Oxford: Alpha Sci. Int. Ltd., 2008.
[54] H. Hellendoorn and C. Thomas, "Defuzzification in fuzzy controllers," *J. Intell. Fuzzy Syst.*, vol. 1, pp. 109–123, 1993.
[55] M. J. Wierman, "Central values of fuzzy numbers - Defuzzification," *Inf. Sci.*, vol. 100, pp. 207–215, 1997.
[56] A. Manuello Bertetto and M. Ruggiu, "Characterization and modeling of air muscles," *Mech. Res. Commun.*, vol. 31, pp. 185–194, 2004.
[57] S. Li, J. Jin, and Q. He, "Modelling and assessment of pneumatic artificial muscle," *Int. J. Eng. Model.*, vol. 19, pp. 95–100, 2006.
[58] A. Boulkroune, M. M'Saad, and M. Farza, "Adaptive fuzzy controller for multivariable nonlinear state time-varying delay systems subject to input nonlinearities," *Fuzzy Sets Syst.*, vol. 164, pp. 45–65.
[59] Z. Fang, D. Xu, and M. Tan, "A vision-based self-tuning fuzzy controller for fillet weld seam tracking," *IEEE/ASME Trans. Mechatronics*, vol. 16, no. 3, pp. 540–550, Jun. 2011.
[60] T. Li, D. Wang, and N. Chen, "Adaptive fuzzy control of uncertain MIMO non-linear systems in block-triangular forms," *Nonlinear Dyn.*, vol. 63, pp. 105–123, 2011.
[61] J. Yu, Y. Ma, B. Chen, and H. Yu, "Adaptive fuzzy tracking control for induction motors via backstepping," *ICIC Exp. Lett.*, vol. 5, pp. 425–431, 2011.
[62] L. Chinn and J. Hertel, "Rehabilitation of ankle and foot injuries in athletes," *Clinics Sports Med.*, vol. 29, pp. 157–167, 2010.
[63] H. P. H. Anh and K. K. Ahn, "Identification of pneumatic artificial muscle manipulators by a MGA-based nonlinear NARX fuzzy model," *Mechatronics*, vol. 19, pp. 106–133, 2009.

Prashant K. Jamwal received the M.Tech. degree from the Indian Institute of Technology, Roorkee, India, and the Ph.D. degree from The University of Auckland, Auckland, New Zealand.

He is an Associate Professor at Rajasthan Technical University, Kota, India, and is pursuing research in biomedical robots, fuzzy mathematics, and multi-objective optimization. He has more than 15 years of teaching and research experience and has published his work in respected journals.

Mr. Jamwal is also an Associate Editor for *the International Journal of Biomechatronics and Biorobotics*.

Sheng Q. Xie (SM'11) received the Ph.D. degrees from the Huazhong University of Science and Technology, Wuhan, China, and the University of Canterbury, Christchurch, New Zealand.

He is the Chair Professor in Mechatronics engineering at The University of Auckland, Auckland, New Zealand. He has more than 20 years of teaching and research experience in mechatronics and robotics. He is the editor of two international journals, and is an editorial board member and scientific advisory member for many international journals and conferences. He has published more than 200 papers in refereed international journals and conferences. His research interests include intelligent mechatronics systems, vision techniques and applications, smart sensors and actuators, Bio-mechatronics and Biomedical robotics.

Shahid Hussain received the B.Sc. degree (Hons.) in mechatronics and control engineering from the University of Engineering and Technology Lahore, Lahore, Pakistan, and the M.E. degree in mechanical engineering from The University of Auckland, Auckland, New Zealand, in 2007 and 2009, respectively. He is currently working toward the Ph.D. degree in the Department of Mechanical Engineering, The University of Auckland.

His research interests include compliant actuation of rehabilitation robots, robot-assisted gait rehabilitation, human–robot interaction, and nonlinear control of dynamic systems.

John G. Parsons received the B.Sc. (Hons.) degree in physiotherapy from Brunel University, London, U.K., the PGDipHSc (Hons.) degree in neurological rehabilitation from Auckland University of Technology, Auckland, New Zealand, and the MHSc (Hons.) degree and the Ph.D. degree in health science from the University of New Zealand, Auckland.

He is a registered physiotherapist with almost 20 years of clinical experience in both the U.K. and New Zealand. He is a Senior Lecturer with Applied Ageing Research Group, Faculty Medical Health Sciences, The University of Auckland. He is committed to the integration of cutting edge engineering innovations into the delivery of health services to patients requiring functional rehabilitation. He is currently a named Investigator on several such collaborative cross-disciplinary projects, including the impact of restricted weight bearing on functional outcomes for older people following lower limb fracture, and the development and user testing of a multilevel system for people with disabilities living at home or in supported accommodation. He continues to lead the clinical trialing of an assistive device among people requiring gait retraining following stroke.